JOURNAL OF OPTOELECTRONICS AND ADVANCED MATERIALS Vol. 10, No. 7, July 2008, p. 1595 - 1600

*Invited paper*

# Effect of chemical composition on ground state properties of Ce and Yb intermetallic compounds

M. GIOVANNINI[a,b], E. BAUER[c], G. HILSCHER[c], H. MICHOR[c], P. ROGL[d], A. SACCONE[a]
[a]*Department of Chemistry, University of Genoa, I-16146 Genoa, Italy*
[b]*LAMIA-INFM-CNR, Corso Perrone 24, I-16152 Genova, Italy*
[c]*Institute of Solid State Physics, University of Technology, A-1040 Vienna, Austria*
[d]*Institute of Physical Chemistry, University of Vienna, A-1090 Vienna, Austria*

The effect of chemical composition on ground state properties of $Ce_2Pd_2In$, $YbCu_4Au$ and $YbCu_4Ag$, showing more or less extended homogeneity ranges, has been shortly reviewed. The ternary indides $Ce_2Pd_{2+2x}In_{1-x}$ and $Ce_{2+x}Pd_2In_{1-x}$ form two branches of solid solutions, and the magnetic properties of these compounds are strongly influenced by composition, which drives the system from ferromagnetic to antiferromagnetic behaviour through the stoichiometric point $Ce_2Pd_2In$. Similarly, $YbCu_4Au$, which is located along the $YbCu_{5-x}Au_x$ solid solution, is at the crossover between two kinds of disordered sublattices, and the ground state properties follow a non-monotonic behaviour through the point of crystallographic order $YbCu_4Au$. $YbCu_4Ag$ is located at one end point of the $YbCu_{5-x}Ag_x$ solid solution and the system exhibits a systematic variation of ground state properties along the solid solution.

(Received April 1, 2008; accepted June 30, 2008)

*Keywords:* Heavy fermion systems, Crystal chemistry of intermetallics, Rare-earth intermetallics

## 1. Introduction

Strong correlation between electrons, due to hybridization of f-electrons and conduction electrons, can cause a number of outstanding low temperature features [1]. Among the rare earths, a large number of these phenomena is found for Ce– and Yb–based compounds which behave, in some respects, in a symmetric way according to the so called electron-hole analogy. Chemical composition, as well as pressure and magnetic field, can play an important role in ground state properties of these compounds. As an example a qualitative scenario, proposed by Doniach [2], is used to understand some of the ground state properties of heavy fermions. In Doniach's scenario two important energy scales are in competition, (i) the inter-site Ruderman-Kittel-Kasuya-Yosida (RKKY) interaction between local moments via the conduction electrons and (ii) the on-site Kondo interaction. The ground state properties of these materials depend on the hybridization, expressed by the parameter $g = |JN(E_F)|$, where J is the conduction-electrons f-electrons exchange constant of the exchange Hamiltonian, and $N(E_F)$ is the conduction-electron density of states at the Fermi energy. For small values of the *g* parameter RKKY interaction dominates, and in this case the ground state of the system will be magnetic. On the other hand, for large values of *g* a Kondo lattice will form with the localized moments completely screened by the conduction electrons. The strength of *g* can be tuned by applying hydrostatic pressure, by changing chemical composition or by using an applied magnetic field. In case of application of pressure and doping, changes of volumes are often the dominant effect in shifting from magnetic to non-magnetic ground states (and vice versa). Composition can be changed by substitution on the Ce or Yb 4f-sites or on the remaining sublattice. In the latter case, replacement can be done with an isoelectronic element (as e.g. in $CeCu_{6-x}Au_x$ or $YbRh_2(Si_{1-x}Ge_x)_2$) or with an element of similar volume but different electronic configuration (as e.g. in $CeIn_{3-x}Sn_x$ or in $YbCu_{5-x}Al_x$). When volume effects play a more important role than electronic effects, it is usual to refer to it as to the application of a "chemical pressure" which will be positive or negative depending on whether the unit cell will reduce or expand.

Regarding the influence of chemical composition on physical properties of intermetallic compounds, an important question to be addressed is whether the compound is a point compound with a fixed composition or it forms in a homogeneity range. In the first case it may be worth investigating the effect of doping with other metals, whereas in the second case an investigation of the homogeneity range of the solid solution is an important prerequisite in order to perform a careful investigation of ground state properties. In fact, it may happen that compounds previously reported to be stoichiometric are later on recognized to be points of crystallographic order of solid solutions.

In the present paper a few examples of compounds which we have recently investigated, namely $Ce_2Pd_2In$ and $YbCu_4T$ (T=Ag, Au, Pd), are discussed in order to illustrate this relevant issue, with the aim to stress the importance of crystallochemistry and compositional phase diagrams for the challenging activity of synthesis and characterization of novel promising materials with strongly correlated electrons.

## 2. Results and discussion

### 2.1 $Ce_2Pd_2In$ and its homogeneity range

This compound belongs to the family of $R_2T_2X$ intermetallics (R = rare earth, T = transition metal, X = p-block element or Mg) crystallizing in the tetragonal $Mo_2FeB_2$ type structure. This structure consists of two different types of atomic planes perpendicular to the **c**-axis, one containing only R atoms and the other built up by T and X atoms. It can also be considered as an intergrowth structure formed by CsCl-type and $AlB_2$-type blocks with a 1:1 ratio, corresponding to slabs of composition RX and $RT_2$, respectively. Each rare earth atom has two nearest R-neighbours along the **c**-axis at a distance corresponding to the lattice parameter *c*. For the $R_2Pd_2In$ series, only one out of five nearest R-neighbours is in the basal plane in a short distance comparable to those in the **c**-direction [3].

*Table 1. Magnetic data obtained on bulk samples of $Ce_2Pd_2In$.*

| $\mu_{eff}(\mu_B/Ce)$ | $\theta_P(K)$ | $T_N$ (K) | $T_C$ (K) | Ref. | Remarks |
|---|---|---|---|---|---|
| | +4 | | 4 | [4] | |
| 2.48 | +18 | | ~ 4.2 | [5] | |
| 2.49 | +12.3 | 4.3 | 4.0 | [7] | Complex magnetic behaviour |
| 2.48* | -22* | 4.5* | 3.7* | [6] | Two magnetic transitions |
| | | | ~3.6 + 3.2? | [8] | Excess Pd lowers magnetic ordering |
| 2.34 | +11 | 4.3 | 3.8 | [3] | Dependence of magnetism on thermal history |

*$CePd_{2.04}In_{0.96}$

From previous literature reports [3-8], considerable discrepancies exist on the nature of magnetic ordering of $Ce_2Pd_2In$. In fact, the issue under discussion was whether only one ferromagnetic ordering at around 4 K occurs [4, 5] or another ordering at around 4.3-4.5 K precedes the FM transition [3,6,7]. Table 1 reports the various magnetic data of $Ce_2Pd_2In$ collected from literature.

In order to shed some light on the ground state properties of this compound, we have performed a careful investigation of its homogeneity range using electron probe microanalysis (EPMA) and X-ray diffraction (XRD) measurements on several samples synthesised in the region around stoichiometry 2:2:1. The result of this study is reported in Fig. 1, showing that $Ce_2Pd_2In$ is located just on the border of a homogeneity field extending in double-branches towards deficiency in indium. One branch (indicated as branch A, of general formula ~ $Ce_2Pd_{2+2x}In_{1-x}$) extends towards the Pd-rich region up to 39 at.% Ce, 47 at.% Pd, 14 at.% In, whereas the other (branch B, of general formula ~ $Ce_{2+x}Pd_2In_{1-x}$) develops in the Ce-rich region up to 49 at. % Ce, 38 at. % Pd, 13 at. % In. The trend of the *c/a* ratio of the lattice parameters versus the off-stoichiometric parameter *x*, is depicted in Fig. 2. The two branches are formed according to a different substitutional mechanism. In fact, whereas in branch B a simple replacement of Ce/In atoms in the 2*a* site of the space group *P4/mbm* occurs, the substitutional process in branch A can be described by a model in which indium vacancies at the 2*a* site are compensated by an excess of palladium located at an additional 4*e* site. These two models were confirmed by quantitative Rietveld refinement of X-ray and neutron powder intensity data carried out on samples of compositions 40 at. % Ce, 45 at.% Pd, 15 at. % In and 47 at. % Ce, 37 at.% Pd, 16 at. % In, respectively. The structural results of the Rietveld profile fitting of the XRD patterns for the two samples belonging to branch A ($Ce_{40}Pd_{45}In_{15}$) and branch B ($Ce_{47}Pd_{37}In_{16}$) are summarised in Table 2.

*Table 2. Structural parameters of $Ce_{40}Pd_{45}In_{15}$ and $Ce_{47}Pd_{37}In_{16}$ refined from neutron-diffraction data taken at T=10 K (space group P4/mbm). Occ.= occupation number, $\chi^2$= goodness of fit, $R_B$= agreement R-Bragg factor, $R_F$= agreement R-structure factor, $R_{WP}$= agreement factor concerning weighed profile intensities, $R_{exp}$= expected value from counting statistic.*

| Sample | Ce in 4*h* (*x*,1/2+*x*, 1/2) | Pd in 4*g* (*x*,1/2+*x*, 0) | In in 2*a* (0,0,0) | Ce in 2*a* (0,0,0) | Pd in 4*e* (0,0,*z*) | R values |
|---|---|---|---|---|---|---|
| $Ce_{40}Pd_{45}In_{15}$ | x=0.1753(1) occ.= 0.98(3) | x=0.3714(1) occ.=1 | occ.=0.86(3) | | z=0.317(3) occ.=0.14(3) | $R_B$=0.0639 $R_F$=0.0517 $R_{WP}$=0.069 $R_{exp}$=0.0351 $\chi^2$=3.94 |
| $Ce_{47}Pd_{37}In_{16}$ | x=0.1730(1) occ.=1 | x=0.3718(1) occ.=1 | occ.=0.60(3) | occ.=0.40(3) | | $R_B$=0.0487 $R_F$=0.0336 $R_{WP}$=0.0498 $R_{exp}$=0.0281 $\chi^2$=3.14 |

*Invited paper*

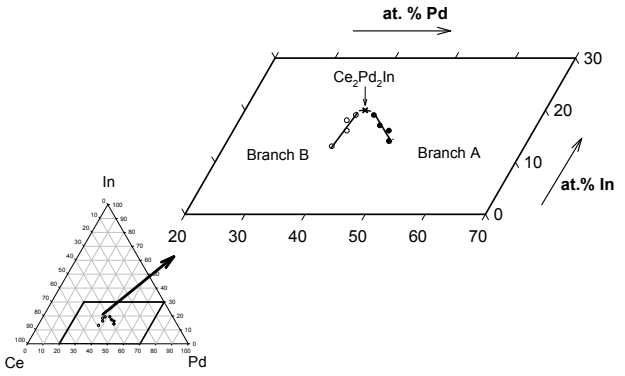


*Fig.1. Location of the two branches (A: $Ce_2Pd_{2+2x}In_{1-x}$; B: $Ce_{2+x}Pd_2In_{1-x}$). The samples prepared along the two branches are indicated by full circles (branch A) and empty circles (branch B).*

The magnetic properties of these indides are strongly influenced by chemical composition. In fact, samples belonging to branch B exhibit ferromagnetic behaviour, whereas in branch A antiferromagnetism occurs ($T_N \sim T_C \approx$ 4 K), as indicated by magnetisation and specific heat measurements and confirmed by neutron diffraction experiments [9]. The magnetic moments in both cases are oriented parallel to the **c** axis, and in case of antiferromagnetism the four Ce magnetic moments are sinusoidally modulated along the **a** axis with a propagation vector **k** ≈ [0.22, 0, 0]. The 2:2:1 composition is just located at the vertex of the two branches i.e. on the edge of antiferromagnetic and ferromagnetic behaviour. Hence, a 2:2:1 sample with some fluctuations of the stoichiometry on a microscopic scale should contain both antiferromagnetic and ferromagnetic domains. This seems to be the reason for the puzzling double effect previously found in the literature for $Ce_2Pd_2In$ [3,6,7]. Furthermore, as a matter of fact, samples prepared at the stoichiometric composition always reveal traces of an extra phase [6, 8]. Thus the two branches may be disconnected by a very narrow two-phase region (as suggested in Fig. 1 by a dashed line).

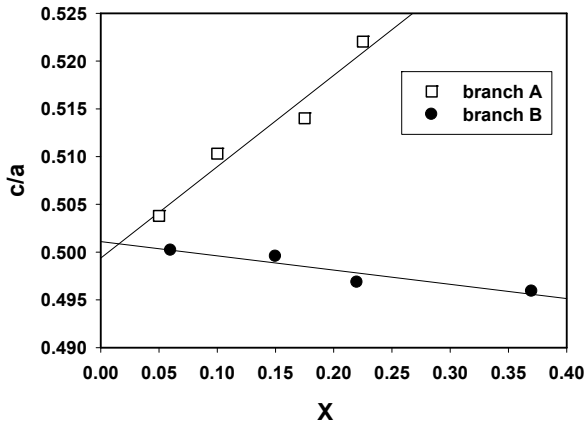


*Fig.2. The variation of the c/a ratio of the lattice parameters at room temperature for the two branches A: $Ce_2Pd_{2+x}In_{1-x}$ and B: $Ce_{2+x}Pd_2In_{1-x}$ as a function of the composition x.*

Searching for differences in crystal chemistry between the two branches, a comparison of the interatomic distances is reported in Tab. 3. Rather short distances $d_{Pd(4e)\text{-}In(2a)}$=2.722 Å for branch A and short distances $d_{Ce(4h)\text{-}Ce(2a)}$=3.505 Å for branch B appear, whereas the remaining sublattices behave indifferently. Thus, the remarkable change of magnetic ordering passing from branch A to branch B is likely caused by differences in RKKY exchange interactions associated with alterations of interatomic distances arising from the substitutional mechanism of the two branches.

*Table 3. Interatomic distances (Å) in $Ce_{40}Pd_{45}In_{15}$ and $Ce_{47}Pd_{37}In_{16}$ calculated from Table 2.*

| $Ce_{40}Pd_{45}In_{15}$ (branch A) | | | | $Ce_{47}Pd_{37}In_{16}$ (branch B) | | | |
|---|---|---|---|---|---|---|---|
| Ce(4*h*)-2Pd(4*g*) | 2.920 | Ce(4*h*)-2Ce(4*h*) | 3.985 | Ce(4*h*)-2Pd(4*g*) | 2.952 | Ce(4*h*)-2Ce(4*h*) | 3.922 |
| Ce(4*h*)-4Pd(4*e*) | 2.932 | Pd(4*g*)-Pd(4*g*) | 2.799 | Ce(4*h*)-4Pd(4*g*) | 3.093 | Pd(4*g*)-Pd(4*g*) | 2.849 |
| Ce(4*h*)-4Pd(4*g*) | 3.094 | Pd(4*g*)-2In(2*a*) | 3.026 | Ce(4*h*)-4Ce/In(2*a*) | 3.505 | Pd(4*g*)-2Ce/In(2*a*) | 3.088 |
| Ce(4*h*)-4In(2*a*) | 3.469 | Pd(4*e*)-Pd(4*e*) | 2.526 | Ce(4*h*)-Ce(4*h*) | 3.842 | Pd(4*g*)-2Pd(4*g*) | 3.922 |
| Ce(4*h*)-Ce(4*h*) | 3.817 | Pd(4*e*)-In(2*a*) | 2.722 | | | | |

### 2.2 $YbCu_4T$ (T=Ag, Au, Pd)

These Yb-based heavy fermion compounds crystallising in the $MgCu_4Sn$ structure, an ordered derivative of the $AuBe_5$-type, were discovered in 1987 in an investigation by Rossel and co-workers [10]. These compounds were reported to exhibit effective electron masses of ~ 60 $m_e$ and, whereas the compounds with T = Au, and Pd order magnetically below 1 K, $YbCu_4Ag$ has a nonmagnetic ground state. Later on, in another study by Severing and co-workers [11], the structure of $YbCu_4X$ (X=Ag, Au) was confirmed to be cubic $AuBe_5$, whereas the Bragg lines of $YbCu_4Pd$ were found to be strongly broadened and reflect some impurity phases. Now it is well established that the first two compounds are not stoichiometric compounds with fixed composition, but rather points of crystallographic order of $YbCu_{5-x}T_x$ (T = Ag, Au) solid solutions [12]. When we started our investigation on these compounds no information was available in literature on the possible formation of an analogous $YbCu_{5-x}Pd_x$ solid solution. In our recent study [12] samples along the section $YbCu_{5-x}Pd_x$ were prepared and characterised by EPMA and XRD. In Fig. 3 the microstructure of $YbCu_4Pd$, showing a multiphase appearance, is reported as a representative of all the samples prepared along the section. Moreover, Fig. 4 shows the X-ray pattern of $YbCu_4Pd$ compared with those of $YbCu_{4.5}$ and $YbCu_{4.8}Au_{0.2}$. This pattern exhibits a general broadening of the Bragg peaks related to the cubic structure and, in addition, the presence of some satellites around the main peaks, similarly to the pattern of binary $YbCu_{4.5}$. The microstructures and XRD patterns of the samples prepared along the $YbCu_{5-x}Pd_x$ section resemble those of the samples in the $0.2 \le x \le 0.4$ region of the section $YbCu_{5-x}Au_x$, where coexistence of the cubic $AuBe_5$-type and its monoclinic superstructure has been observed [12] (see Fig. 4). Thus, our results indicate that $YbCu_4Pd$, as well as the samples of the section $YbCu_{5-x}Pd_x$, do not form as cubic single phase, but mainly appear as a mixture of cubic $AuBe_5$ and the very complex monoclinic superstructure formed in $YbCu_{4.5}$.

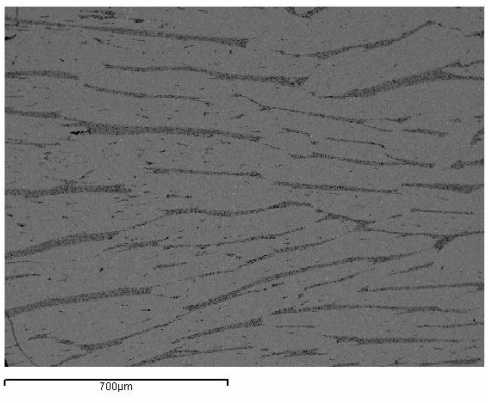


*Fig. 3. Scanning electron micrograph of $YbCu_4Pd$ annealed at 600 °C for 20 days.*

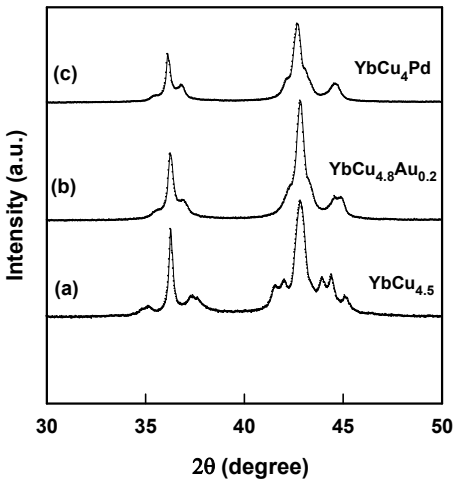


*Fig. 4. X-ray diffraction (Cu $K_\alpha$) powder patterns of (a) $YbCu_{4.5}$; (b) $YbCu_{4.8}Au_{0.2}$ and (c) $YbCu_4Pd$.*

$YbCu_4Ag$ and $YbCu_4Au$ form ordered lattices where Yb, Cu and Ag (Au) atoms are located on the 4*a*, 16*e* and 4*c* crystallographic sites of the $F\bar{4}3m$ space group, respectively. Substitution of Ag (Au) by Cu in the 4*c* site retains the cubic $AuBe_5$ structure forming extended solid solutions $YbCu_{5-x}T_x$ (T=Ag, Au) up to values of $1 \ge x \ge 0.125$ and $1 \ge x \ge 0.4$ for Ag and Au, respectively (see Fig. 5, where the homogeneity ranges of $Yb(Cu,Ag)_5$ and $Yb(Cu,Au)_5$ are compared). Further T/Cu replacement stabilises the monoclinic superstructure based on $YbCu_{4.5}$. In fact, in the Yb-Cu system at ambient pressure $YbCu_{4.5}$ rather than $YbCu_5$ is formed [12]. Starting again from the $YbCu_4T$ ordered lattice, replacement of Cu by Ag (Au) retains the $AuBe_5$ structure only in the case of Au (in the 16*e* site) up to $x$=1.8. For further Cu/Au substitution (from 31 to 40 at.% Au) the cubic phase becomes unstable and the monoclinic superstructure is formed. In the case of Ag, samples prepared in the range $1 < x < 1.8$ of the $YbCu_{5-x}Ag_x$ section were not single phase and, as a consequence, $YbCu_4Ag$ is located at one border of the homogeneity range of the solid solution (see Fig. 5). On the other hand, $YbCu_4Au$ marks the crossover between two kinds of disordered sublattices, from the $0 < x < 1$ region where Cu/Au replacement at the 4*c* site occurs, to the $1 < x < 1.8$ range with Cu/Au substitution at the 16*e* site [13]. Thus, the physical properties are expected to show distinct features as $x$ is varied through $x$=1 in $YbCu_{5-x}Au_x$. $YbCu_4Au$ exhibits long-range magnetic order at $T_N$ = 0.6 K, with the magnitude of the magnetic moments involved in the ordering process reduced by the Kondo effect [14]. Figure 6 reports the isothermal magnetoresistance at T= 2K of $YbCu_{5-x}Au_x$ as a function of magnetic field for various concentrations. It is worth noting that for all samples the magnetoresistance is negative, and that its

magnitude decreases either on replacing Cu by Au at 16*e* ($1<x<1.8$) or by substitution of Au by Cu at 4*c* ($1>x>0.4$). An analysis of the magnetoresistance data in terms of the Schlotmann-Batlogg model [15] yields the lowest value of the Kondo temperature $T_K$ for the ordered compound $YbCu_4Au$ ($T_K$ = 1 K) with an increase of the Kondo temperature by both types of alloying [13]. Therefore, starting from $YbCu_4Au$, in the isoelectronic substitution of Cu atoms by the bigger Au atoms at the 16*e* site, volume effects seem to dominate electronic effects, hybridisation increases and the ground state of the system shifts towards stronger Kondo interactions in line with the Doniach scenario. On the other hand, replacing Au atoms by the smaller Cu atoms at the 4*c* site of $YbCu_4Au$, electronic effects seem to play a more important role than volume effects and thus chemical substitution cannot be simulated by an increasing hydrostatic pressure.

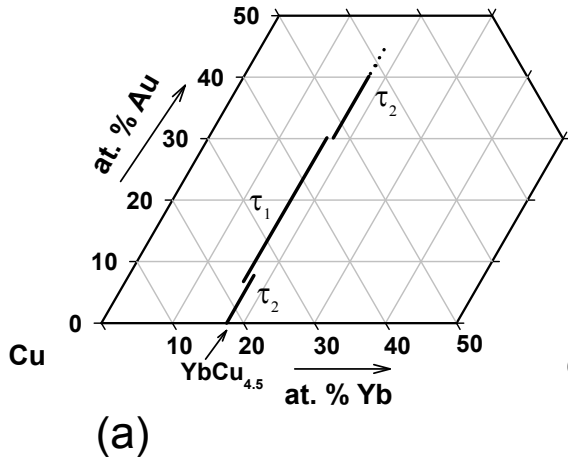


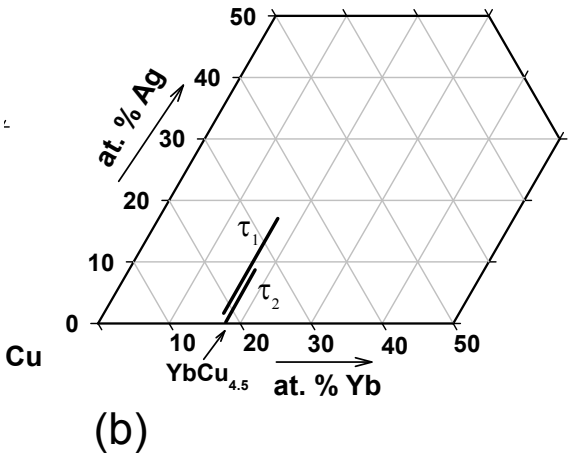


*Fig. 5. Schematic compositional phase diagrams showing the homogeneity ranges of Cu-rich solid solutions in the (a) Yb-Cu-Au system and in the (b) Yb-Cu-Ag system. $\tau_1$= cubic $AuBe_5$-type; $\tau_2$= monoclinic $YbCu_{4.5}$-based phase.*

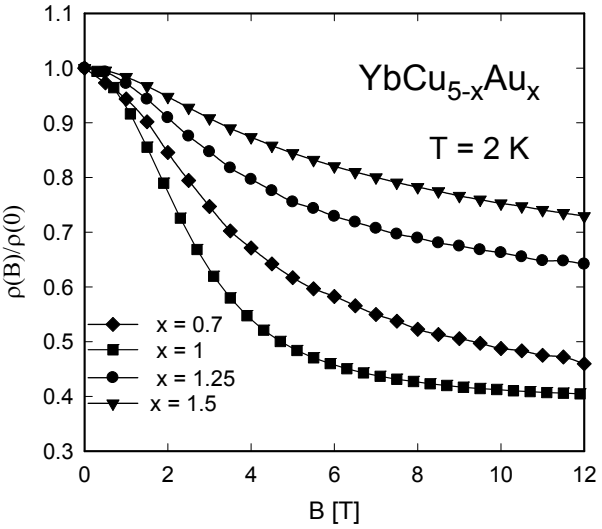


*Fig. 6. The isothermal magnetoresistance $\rho(B)/\rho(0)$ of $YbCu_{5-x}Au_x$ for various concentrations x at T=2 K. $\rho(B)$ and $\rho(0)$ are the resistivities at a magnetic field B and at zero field, respectively.*

The ground state of $YbCu_4Ag$ is surprisingly different from that of $YbCu_4Au$. It exhibits an unusual large Kondo temperature ($T_K$ = 150 K), exceeding both RKKY Kondo interaction as well as crystal-field splitting [16]. Differently from the case of Au, the isoeletronic substitution of Ag atoms by the smaller Cu atoms at the 4*c* site simulates quite well the effect of hydrostatic pressure. The system exhibits Kondo lattice behaviour in the $1\geq x>0.125$ substitutional range with a systematic variation of characteristic quantities such as the Kondo temperature, the coefficient of electronic specific heat and the Pauli paramagnetic susceptibility [16,17].

## 3. Conclusions

The effect of chemical composition on ground state properties of $Ce_2Pd_2In$, $YbCu_4Au$ and $YbCu_4Ag$, showing more or less extended homogeneity ranges, has been shortly reviewed. Starting from the 2:2:1 stoichiometry, the ternary indides form two branches of solid solutions due to different substitutional mechanisms. The magnetic properties are strongly influenced by the chemical composition. Excess of Pd induces antiferromagnetism of a sinusoidal modulated type, whereas excess of Ce favours ferromagnetism. $Ce_2Pd_2In$ is just located on the verge of antiferromagnetic and ferromagnetic behaviour. Similarly, $YbCu_4Au$ is at the crossover between two kinds of disordered sublattices and ground state properties follow a non-monotonic behaviour through this point of crystallographic order. Although the Cu/Au substitution is isoelectronic, $T_K$ exhibits the lowest value for the $YbCu_4Au$ ordered compound, and Kondo interaction increases for both $1>x>0.4$ and $1<x<1.8$ branches of the $YbCu_{5-x}Au_x$ solid solution. $YbCu_4Ag$ is located at one end

point of the $YbCu_{5-x}Ag_x$ solid solution ($1 \geq x > 0.125$). Differently from the case of Au in the analogous region ($1 \geq x > 0.4$), the Ag/Cu isoelectronic substitution simulates quite well the effect of hydrostatic pressure. Finally, $YbCu_4Pd$ has been found to appear as a mixture of two phases: the cubic $AuBe_5$-type and its monoclinic superstructure ($YbCu_{4.5}$ type).

**Acknowledgements**

Part of this work was done within the framework of the thematic subject "Emergent Behaviour in Correlated Matter" (ECOM) of the European Research Project COST P16, which is acknowledged for financial support.

## References

[1] G. R. Stewart, Rev. Mod. Phys. **73**, 797 (2001).
[2] S. Doniach, Physica **91B**, 231 (1977).
[3] M. Giovannini, H. Michor, E. Bauer, G. Hilscher, P. Rogl, R. Ferro, J. Alloys Comp. **280**, 26 (1998).
[4] F. Hulliger, B. Z. Hue, J. Alloys Comp. **215**, 267 (1994).
[5] R. A. Gordon, Y. Ijiri, C. M. Spencer, F. J. DiSalvo, J. Alloys Comp. **224**, 101 (1995).
[6] F. Fougeout, P. Gravereau, B. Chevalier, L. Fournès, J Etourneau, J. Alloys Comp. **238**, 102 (1996).
[7] D. Kaczorowski, P. Rogl, K. Hiebl, Pys. Rev. B **54**, 9891 (1996).
[8] R. Mallik, E. V. Sampathkumaran, J. Dumschat, G. Wortmann, Sol. State Comm. **102**, 59 (1997).
[9] M. Giovannini, H. Michor, E. Bauer, G. Hilscher, P. Rogl, T. Bonelli, F. Fauth, P. Fischer, T. Herrmannsdörfer, L. Keller, W. Sikora, A. Saccone, R. Ferro, Phys. Rev. B **61,** 4044 (2000).
[10] C. Rossel, K. N. Yang, M.B. Maple, Z. Fisk, E. Zirngiebl, J. D. Thompson, Phys. Rev. B **35**, 1914 (1987).
[11] A. Severing, A.P. Murani, J.D. Thompson, Z. Fisk, C. K. Loong, Phys. Rev. B **41**, 1739 (1990).
[12] M. Giovannini, R. Pasero, S. De Negri, A. Saccone, Intermetallics (2007), doi:10.1016/j.intermet.2007.11.010 (in press).
[13] M. Giovannini, A. Saccone, St. Müller, H. Michor, E. Bauer, J. Phys: Condens Matter **17**, S877 (2005).
[14] E. Bauer, E. Gratz, R. Hauser, Le Tuan, A. Galatanu, A. Kottar, H. Michor, W. Perthold, G. Hilscher, Phys. Rev. B **50** 9300 (1994).
[15] P. Schlotmann, Z. Phys. B **51**, 223 (1983).
[16] H. Michor, K. Kreimer, N. Tsujii, K. Yoshimura, K. Kosuge, G. Hilscher, Physica B **319**, 277 (2002).
[17] K. Yoshimura, N. Tsujii, J. He, M. Kato, K. Kosuge, H. Michor, K. Kreiner, G. Hilscher, T. Goto, J. Alloys Compounds **262/263**, 118 (1997).

*Corresponding author: giovam@chimica.unige.it